Electronic Supplementary Information

I.A- Explicit expressions for the MQQT phase shift, flux normalized scattering amplitude, DCSs and ICSs.

The MQQT phase shift is defined (as in RQQT, but distinct from QM) as the phase difference between (1) the path of the incoming wave $\boldsymbol{k}$ which is (inelastic) scattered from the shell at the impact position $R_S^{\mathrm{mod}}(\cos\gamma_a;\cos\beta)$ into an outgoing wave $\boldsymbol{k}'$ and (2) the virtual reference path in which the incoming wave $\boldsymbol{k}$ is scattered at $R_S = 0$ into an unperturbed out going wave $\boldsymbol{k}'$ which leads to[1]

$$\eta^{\mathrm{mod}}_{j=0.5\to j'}(\gamma_a;\beta,p) = -\boldsymbol{a}(\beta,p)\cdot\boldsymbol{R_S^{mod}}(\cos\gamma_a;\beta) = K(\beta,p)\times R^{\mathrm{mod}}_{S\perp}(\gamma_a;\beta) \tag{I.1}$$

in which,

$$K(\beta,p)\equiv[k_\perp+(-1)^{p-1}\times k'_\perp] = |k\times\cos\beta| + (-1)^{p-1}\sqrt{|k\times\cos\beta|^2 - \tfrac{2\mu}{\hbar^2}E_{j'}} \tag{I.2}$$

the so called kinetic factor, which depends only on p and β and

$$R^{\mathrm{mod}}_{S\perp}(\gamma_a;\beta)\equiv\hat{\boldsymbol{a}}(\gamma_a)\cdot\boldsymbol{R_S^{mod}}(\cos\gamma_a;\beta) = R_S^{\mathrm{mod}}(\cos\gamma_a;\beta)\times\cos(\gamma_R-\gamma_a) \tag{I.3}$$

denotes the surface normal projected PES contour radius vector, which depends both on γ_a and β in the case of MQQT and solely on γ_a in the case of RQQT because $R^{reg}_{S\perp}(\cos\gamma_a)\equiv R^{\mathrm{mod}}_{S\perp}(\cos\gamma_a;\beta=180°)$.

Note that only paths (differentiated by the polar angle γ_a) from an initial and to a final rotational state scattered into the same β, p and ϕ_a apse frame parameters, are allowed to interfere with each other. Eqs (I.1-I.3) jointly imply:

$$\eta^{\mathrm{mod}}_{j=0.5\to j'}(\gamma_a;\beta,p=2) = \frac{|\cos\beta|-\sqrt{\cos^2\beta - E_{j'}/E_{col}}}{|\cos\beta|+\sqrt{\cos^2\beta - E_{j'}/E_{col}}}\times\eta^{\mathrm{mod}}_{j=0.5\to j'}(\gamma_a;\beta,p=1) \tag{I.4}$$

The apse frame MQQT scattering amplitude follows as:

$$g^{\mathrm{mod}}_{j=0.5,m_a,\bar{\Omega}=0.5,\varepsilon\to j',m'_a,\bar{\Omega}'=0.5,\varepsilon'}(\beta,p) =$$

$$=<j',m'_a,\bar{\Omega}'=0.5,\varepsilon'|\,g^{\mathrm{mod}}_{geom}(\gamma_a;\beta)\times\exp[i\eta^{\mathrm{mod}}_{E=0\to E(j')}(\gamma_a;\beta,p)]\,|\,j=0.5,m_a,\bar{\Omega}'=0.5,\varepsilon> \tag{I.5}$$

The MQQT fixed-molecule scattering amplitude for a particular j=0.5 to j' transition,

extends from that of a RQQT fixed-molecule transition:[1]

$$g^{\mathrm{mod}}_{E=0\to E(j')}(\gamma_a;\beta,p) = g^{\mathrm{mod}}_{geom}(\gamma_a;\beta)\times\exp[i\eta^{\mathrm{mod}}_{j=0.5\to j'}(\gamma_a;\beta,p)] \tag{I.6}$$

where

$$g^{\mathrm{mod}}_{geom}(\gamma_a;\beta) = \sqrt{|\cos\beta|\times\rho^{\mathrm{mod}}_1(\gamma_a;\beta)\times\rho^{\mathrm{mod}}_2(\gamma_a;\beta)} \tag{I.7}$$

denotes the geometric scattering amplitude. The MQQT hard shell principal radii of curvature $\rho^{\mathrm{mod}}_1(\gamma_a;\beta)$ and $\rho^{\mathrm{mod}}_2(\gamma_a;\beta)$ differ from the RQQT values by depending on β, while the MQQT phase shift $\eta^{\mathrm{mod}}_{j=0.5\to j'}(\gamma_a;\beta,p)$ exhibits a different dependence on β.[2, 3]

To obtain the MQQT apse frame scattering amplitude, the product of $g^{\mathrm{mod}}_{E=0\to E(j')}(\gamma_a;\beta,p)$ and $\Psi^*_{j',m_a,\varepsilon'}(\gamma_a,\phi_a)\times\Psi_{j=0.5,m_a,\varepsilon}(\gamma_a,\phi_a)$ is integrated over the full range of the spherical angles of the molecular axis (γ_a and ϕ_a):

$$g^{\mathrm{mod}}_{j=0.5,m_a,\varepsilon\to j',m'_a,\varepsilon'}(\beta,p) \equiv \int_0^{2\pi} d\varphi_a \int_{-1}^{1} d\cos\gamma_a \times g^{\mathrm{mod}}_{E=0\to E(j')}(\gamma_a;\beta,p)\times\Psi^*_{j',m'_a.\varepsilon'}(\gamma_a,\varphi_a)\times\Psi_{j=0.5,m_a.\varepsilon}(\gamma_a,\varphi_a) \tag{I.8}$$

It is only when that $m_a = m'_a$ the integral of the product of the NO rotational wave functions of Eq.(I.8) is not necessarily equal to zero. The product of the two wavefunctions can be contracted to[2, 3]

$$\Psi^*_{j',m_a,\varepsilon'}(\gamma_a,\varphi_a)\times\Psi_{j=1/2,m_a,\varepsilon}(\gamma_a,\varphi_a)\times\delta_{m_a,m'_a} = \tfrac{1}{4\pi}\sqrt{j'+\tfrac{1}{2}}\times P_{j'-\varepsilon\cdot\varepsilon'/2}(\cos\gamma_a)\times\left[m_a/|m_a|\right]^{(1-\varepsilon\cdot\varepsilon')/2} \tag{I.9}$$

Note that the m_a conserving Eq. (I.9) is proportional to the Legendre polynomial $P_n(\cos\gamma_a)$ where n denotes the parity pair number

$$n \equiv j' - \varepsilon\times\varepsilon'/2 \tag{I.10}$$

Consequently the dependence upon β and p of the ε = -1, j = ½ MQQT DCSs scattered into the parity pair ε' =1, $j' = n - 0.5$ and ε' = -1, $j' = n + 0.5$ rotationally excited states are similar.[2-10] The rotationally inelastic apse frame DCS corresponding to scatterings from the $j=\frac{1}{2}$, $m_a=\frac{1}{2}$, ε initial rotational quantum into the $j', m_a=\frac{1}{2}, \varepsilon'$ rotationally exited quantum state is then given by

$$\frac{d\sigma^{\mathrm{mod}}_{j=0.5,\varepsilon\to j',\varepsilon'}}{d\omega_a}(\beta,p) = |\sqrt{C^{\mathrm{mod}}_{norm}}\times g^{\mathrm{mod}}_{j=0.5,\varepsilon\to j',\varepsilon'}(\beta,p)|^2 \tag{I.11}$$

where C^{mod}_{norm} denotes the normalization factor which ensures that the total collision cross section summed over all the rotational states is equal to the geometric ICS

$$C_{norm}^{\mathrm{mod}} \equiv \frac{\int_0^{2\pi} d\varphi \int_{-1}^{0} d\cos\beta \cdot d\sigma_{geom}^{\mathrm{mod}}(\beta)/d\omega_a}{\sum_{j',\varepsilon',p} \int_0^{2\pi} d\varphi \int_{-1}^{0} d\cos\beta \cdot |\, g_{j=0.5,m_a,\varepsilon\to j',m_a,\varepsilon'}^{\mathrm{mod}}(\beta,p)\,|^2} \tag{I.12}$$

where the geometric DCS in the case of $j=\frac{1}{2}$ follows from

$$\frac{d\sigma_{geom}^{\mathrm{mod}}}{d\omega_a}(\beta) \equiv \frac{1}{2}\int_{-1}^{1} d\cos\gamma_a \cdot [g_{geom}^{\mathrm{mod}}(\gamma_a;\beta)]^2 \tag{I.13}$$

The integral quantum state resolved rotationally inelastic modified QQT ICS is given by

$$\sigma_{j=0.5,\,\varepsilon\to j',\,\varepsilon'}^{\mathrm{mod}} = 2\pi \sum_p \int_{-1}^{0} d\cos\beta \cdot \frac{d\sigma_{j=0.5,\,\varepsilon\to j',\,\varepsilon'}^{\mathrm{mod}}}{d\omega_a}(\beta,p) \tag{I.14}$$

To transform a MQQT or RQQT apse frame DCS into a collision frame DCS one employs:[1]

$$\frac{d\sigma_{j=\frac{1}{2},\varepsilon\to j',\varepsilon'}}{d\omega}(\theta) = \frac{d\sigma_{j=\frac{1}{2},\varepsilon\to j',\varepsilon'}}{d\omega_a}(\beta,p) \times \left|\frac{d\cos\beta}{d\cos\theta}\right| = \frac{d\sigma_{j=\frac{1}{2},\varepsilon\to j',\varepsilon'}}{d\omega_a}(\beta,p) \times \frac{(k')^2\,|\,k'-k\cos\theta\,|}{[(k')^2-2k'k\cos\theta+k^2]^{1.5}} \tag{I.15}$$

The smallest scattering angle $\theta=\theta_\kappa$ of the $p\equiv 1$ range for which $\frac{d\sigma_{i\to f}}{d\omega}(\theta)$ remains classically allowed matches the largest scattering angle θ of the classically forbidden $p\equiv 2$ range. At $\theta=\theta_\kappa$ $\left|\frac{d\cos\beta}{d\cos\theta}\right|=0$ and so $\frac{d\sigma_{i\to f}}{d\omega}(\theta)=0$.[1] Moreover the classically forbidden but Feynman path allowed $p\equiv 2$, θ range gives rise to a sharp maximum of all rotationally inelastic QQT DCSs at $\theta=0$ because the denominator of Eq. (I.15) reaches its minimum, $[k-k']^2$. The value of $\theta>0$ at which the QQT DCSs maximizes again increases with j'.[1] The forward peaking in the classically forbidden region at $\theta=0$ of all MQQT and RQQT DCSs is an unphysical artifact especially for $j'>\frac{5}{2}$. The exclusion of the p=2 classically forbidden region leads only to a 4.3% increase of the (close to unity) value of $C_{norm}^{\mathrm{mod}}=1.276$ $\sigma_{geom}^{Mod}=0.2414\,(\text{Å}^2)$ and to an even smaller 3.1% raise of the RQQT counterpart value $C_{norm}^{reg}=1.238$ and $\sigma_{geom}^{reg}=0.2121\,(\text{Å}^2)$.

I.B- Legendre expansion coefficients

The Legendre expansion coefficients of a contour of the V_{sum} PES $R_S^{Mod}(\gamma_a;\beta)$ were numerically obtained from Eq. (I.16) below or from Eqs (II.2) and (II.9),

$$C_n(\cos\beta) \equiv \tfrac{2n+1}{2}\int_{-1}^{1} d\cos\gamma_a \cdot R_S^{Mod}(\gamma_a;\beta)\cdot P_n(\cos\gamma_a) \qquad \text{(I.16)}$$

Eq.(I.16) applies to the case of a smooth convex MQQT PES contour for which the functionality $\gamma_R(\gamma_a)$ is valid, which holds for all MQQT He-NO(X) PES contours with $\beta \geq \beta_{\min}^{convex} = 101.45°$. The partially concave contours of the He-NO(X) hard shell PES in the case of $90° \leq \beta < \beta_{\min}^{convex} = 101.45°$ are reminiscent of the so called "rabbit ears" that dominate the softer repulsive parts of the full NO-He PESs.[11] The node between these "ears" near $\cos\gamma_R \approx 0$ corresponds to the node of the π* lobe of the anti-bonding unpaired electron orbital of the NO molecule.[11]

The one electron π* lobe charge density is deemed to be much lower than that provided by the closed shell electrons of the NO(X) molecule. This leads to a Pauli repulsion softening at the π* lobe parts of the He-NO(X) PES, which remains absent at the node of the π* lobe at $\cos\gamma_R \approx 0$. The Legendre expansion coefficients in this example of partially concave contours were obtained numerically by the choice of a proper integration path specified by Eqs (II.1) and (II.2). The vertical dotted lines in each panel of Fig. A indicate the minimum value of $E_{col}\times\cos^2\beta$, at which a $\Delta j \equiv j' - \frac{1}{2}$ transition becomes energetically allowed. The particular value of $E_{col}\times\cos^2\beta$ at which each Δj transition becomes allowed is indicated below the horizontal axis, and the corresponding apse angle β is shown just above the upper horizontal axis. The $C_{n>0}(\beta)$ curves depicted in Fig. A range between about -0.3 and 0.69 Bohr. All $C_n(\beta)$ curves were found to depend most strongly on β in the concave range $90° \leq \beta < \beta_{\min}^{convex} = 101.45°$. The $C_n(\beta)$ curves become nearly stationary for larger β or exhibit a weak linear slope in their dependence upon $\cos^2\beta$. The low order even C_2 and C_4 and odd C_1 and C_3 coefficients, are the dominating anisotropic coefficients of the NO(X, v = 0)-He MQQT shell PES. Note that the actual value of the (by far largest) C_0 coefficient relates solely to the rotationally elastic scattering DCS. Its actual value is irrelevant for the sought

after rotationally inelastic MQQT DCSs.

In the "low" perpendicular collision energy range $0 \le E_{col} \times \cos^2\beta < 20\ cm^{-1}$ which includes collisions that probe partially concave PES contours, the absolute values of the four dominant C_n hard shell Legendre coefficients decrease rapidly if $E_{col} \times \cos^2\beta$ increases. Note that at this particular range it is only the $\Delta j \le 2$ inelastic DCSs that are energetically allowed. In more detail, the prescription of Eq.(2) restricts the probing range of the partially concave V_{sum} PES contours to: $E_{col} \times \cos^2\beta < 20\ cm^{-1}$, $5.016\ cm^{-1} \le E_{col} \times \cos^2\beta < 20\ cm^{-1}$ and $13.38\ cm^{-1} \le E_{col} \times \cos^2\beta < 20\ cm^{-1}$ respectively for the $\Delta j = 0$, $\Delta j = 1$ and $\Delta j = 2$ (in)elastic DCSs. All $C_{n=j'-\varepsilon\varepsilon'/2}(\cos\beta)$ expansion coefficients obtained in this lower PES concave range of $0 \le E_{col} \times \cos^2\beta \le 20\ cm^{-1}$ were found to join perfectly with those obtained from the "upper" PES contour range $20\ cm^{-1} \le E_{col} \times \cos^2\beta \le 508\ cm^{-1}$. As can be seen from Fig. A, at this upper range, the C_2 and also the much smaller valued C_5 and C_6 coefficients remain nearly constant, while the absolute values of C_1 and C_3 and C_4, decrease with increasing $\cos^2\beta$. Moreover, by definition at $\cos^2\beta = 1$ the MQQT C_n coefficients are identical to those of RQQT.

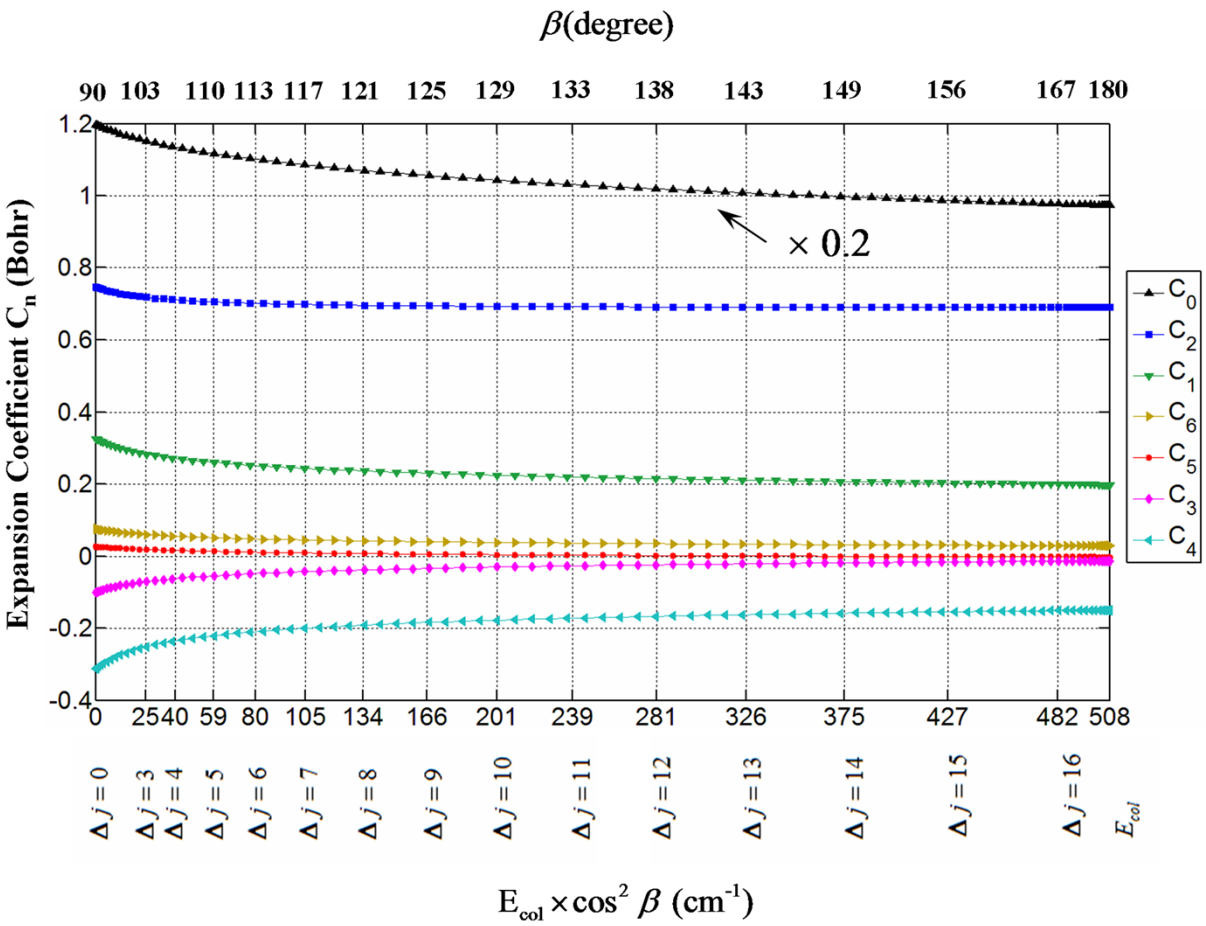

Figure A. The dependence of the modified QQT Legendre polynomial expansion coefficient $C_n(\cos\beta)$ of NO(X)-He at E_{col} =508 cm^{-1} on the fraction of the collision energy available for rotational excitation $E_{col}\cdot\cos^2\beta$. The dashed vertical lines denote the energetic threshold at which the rotationally inelastic transition Δj is energetically allowed. Note that the upper horizontal scale marks also the values of β. In the case of $\Delta j \cong 0$ and $\varepsilon' = \pm\varepsilon$ at one has $\theta \cong 2\beta - \pi$.[3]

II. The Legendre moments and the scattering amplitude of a partially concave shell

To apply the MQQT and RQQT of the rotationally inelastic collision problem onto a partially concave PES contours eqs (I.2) and (I.3) do not suffice. As was already noted in Section 2, the He-NO(X) PES contours given by

$$V\{R_S^{\mathrm{mod}}[\cos\gamma_a(\cos\gamma_R);\beta]\} = E_{col}\times\cos^2\beta \qquad \text{(II.1)}$$

turn out to be partially concave for $90^\circ \le \beta < \beta_{\min}^{convex} = 101.45^\circ$.

For convenience we define the generalized function

$$F[\cos\gamma_a(\cos\gamma_R);\beta,p,j',m_a,\varepsilon',\varepsilon,n] \equiv g^{\mathrm{mod}}_{E=0\to E(j')}(\gamma_a;\beta,p)\times\Psi^*_{j',m_a,\varepsilon'}(\gamma_a,\varphi_a)\times\Psi^*_{j=0.5,m_a,\varepsilon}(\gamma_a,\varphi_a) \qquad \text{(II.2)}$$

and

$$F[\cos\gamma_a(\cos\gamma_R);\beta,p=0,j',m_a,\varepsilon',\varepsilon,n] \equiv \tfrac{2n+1}{2}R_S^{Mod}(\gamma_a;\beta)\times P_n(\cos\gamma_a) \qquad \text{(II.3)}$$

which represent respectively the integrand of eqs (I.8) in the range of $90° \le \beta \le \beta_{\min}^{convex}$.

A concave curvature maximum occurs for the particular $\gamma_a(\gamma_R^{waist})$ at which

$$\frac{d\cos\{\gamma_a[\cos\gamma_R]\}}{d\cos\gamma_R}=0\,,\ \frac{d\cos\{\gamma_a[\cos\gamma_R-\Delta]\}}{d\cos\gamma_R}<0 \text{ and } \frac{d\cos\{\gamma_a[\cos\gamma_R+\Delta]\}}{d\cos\gamma_R}>0 \qquad \text{(II.4)}$$

,where Δ denotes an arbitrary positive infinitesimal small number. Convening to the definition given in Section 3.1 this (local) concave curvature maximum is called a "waist" for brevity. In our NO(X) + He example there is maximally up to one such waist permitted for each of the $0 < V_{sum} \le 508\ cm^{-1}$ PES contours. The functionality $\cos\gamma_a(\cos\gamma_R)$ for the example of β = 90°, depicted in Fig. B, shows that the PES contour $R_S^{\mathrm{mod}}(\cos\gamma_R;\beta=90°)$ exhibits a concave interval that ranges from $\cos\gamma_R=-0.1219$ to $\cos\gamma_R=0.1482$ or from $\gamma_R=97.00°$ to $\gamma_R=81.59°$ at which $\cos\gamma_a$ varies between $\cos\gamma_a=-0.0855$ and $\cos\gamma_a=-0.0933$ or γ_a between 94.90º and 81.59º. Note this concave range covers a ≈5.5° range of γ_R, at which γ_a varies by only 0.45°. Moreover note that the selected β=90º apse angle of Fig. B designates the extreme case of a glancing collision which scatters into θ = 0 direction, for which only the $\Delta j=0,\ \varepsilon\to\varepsilon'=-1$ transition is classically allowed. Eq.(2) shows that for kinematic reasons the apse angle β range which permits the $j=\frac{1}{2}\to j'$ rotational transition MQQT restricts its impact onto hard shell PES contours for which:

$$-1\le\cos\beta\le\cos\beta_\kappa(j')\equiv-\sqrt{E(j')/E_{col}} \qquad \text{(II.5)}$$

Since the $R_S^{\mathrm{mod}}(\cos\gamma_R;\cos\beta)$ contours were found to be purely convex only if $\beta\ge\beta_{\min}^{convex}=101.45°$ or $\cos\beta\le\cos\beta_{\min}^{convex}=-0.2079$, the range of partially concave PES contours is limited to $-0.2079<\cos\beta\le\cos\beta_\kappa(j')\equiv-\sqrt{E(j')/508\ cm^{-1}}$ or

$$\arccos\left(-\sqrt{E(j')/508\ cm^{-1}}\right)\le\beta<\beta_{\min}^{convex}=101.45° \qquad \text{(II.6)}$$

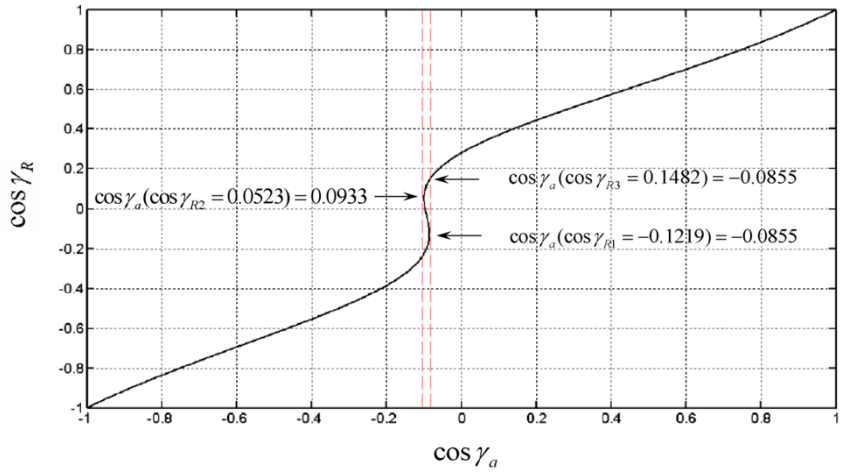

Figure B. The relation between $\cos\gamma_a$ and $\cos\gamma_R$ of the modified He-NO(X) hard shell contour $R_S^{\mathrm{mod}}(\cos\gamma_R;\cos\beta=0)$ given by $V_{sum}\left(R,\gamma_R\right)=0$. The concave waist of this particular contour is the largest one among the modified shell contours of the He-NO(X) collision system. The function $\cos\gamma_a(\cos\gamma_R)$, as shown in the figure, reaches a local maximum $\cos\gamma_{a,\max}=-0.0855$ (indicated by a red dashed vertical line) at $\cos(\gamma_R)\equiv\cos(\gamma_{R_1})=-0.1219$ (indicated by a black horizontal arrow). Thereafter $\cos\gamma_a(\cos\gamma_R)$ decreases monotonically till $\cos\gamma_{R2}=0.0523$ (indicated by a black arrow) a local minimum $\cos\gamma_{a,\min}=-0.0993$ (indicated by a red dashed vertical line) is reached. Having passed this minimum $\cos\gamma_a(\cos\gamma_R)$ increases monotonically passing the local maximum $\cos\gamma_{a,\max}=-0.0855$ at $\cos\gamma_{R3}=0.1482$ to its largest allowed value of $\cos\gamma_R=1$. Concave waists in the He-NO(X) contours persist up to $R_S^{\mathrm{mod}}[\cos\gamma_R;\cos(\beta=102°)]=-0.208$.

Since $\cos\beta_\kappa(j'=\frac{1}{2})=0$, $\cos\beta_\kappa(j'=\frac{3}{2})=-0.0995$ and $\cos\beta_\kappa(j'=\frac{5}{2})=-0.1626$ are all larger than and $\cos\beta_k(j'=\frac{5}{2})=-0.2227$ is smaller than $\cos\beta_{\min}^{conv}=-0.2079$, only the rotationally (in)elastic DCSs to the $j'=\frac{1}{2}$, $j'=\frac{3}{2}$ and $j'=\frac{5}{2}$ final rotational states, are influenced by the concave part of a PES contours at forward scattering angles with $\cos\beta>-0.2079$. Upon the substitution of Eq. (2) into Eq.(3) one obtains:

$$\cos\theta_\kappa=\sin\beta_\kappa \tag{II.7}$$

The substitution of the values $\cos\beta_k(j'\le\frac{5}{2})$ into Eq. (II.7) results in collision frame cutoff angles of $\theta_\kappa(j'=\frac{1}{2})=0°$, $\theta_\kappa(j'=\frac{3}{2})=5.71°$ and $\theta_\kappa(j'=\frac{5}{2})=9.36°$.

As the modified hard shell PES is partially concave in the range $90°\le\beta<101.45°$ provisions have to be taken to ensure that $R_S^{\mathrm{mod}}[\cos\gamma_a(\gamma_R);\beta]$ is assigned to a unique value of $\cos\gamma_a$. To meet this requirement, as shown for the β=90º example of Fig. B, the modified QQT hard shell PES, 3, is divided into the following intervals of $\cos\gamma_a$:

a) $-1\le\cos\gamma_a(\gamma_R)\le\cos\gamma_a[\cos\gamma_{R1}(\beta)]$
Where $\cos\gamma_a[\cos\gamma_{R1}(\beta;\mathrm{j}')]$ denotes the local maximum of $\cos\gamma_a$ that occurs at $\cos\gamma_{R1}(\beta=90°)=-0.1219$ in Fig. B, which shifts towards a larger value when one increases β. The first local maximum disappears if $\beta>102°$.

b) $\cos\gamma_{a,}[\cos\gamma_{R1}(\beta)]>\cos\gamma_a(\gamma_R)\ge\cos\gamma_a[\cos\gamma_{R2}(\beta)]$
Where $\cos\gamma_a[\cos\gamma_{R2}(\beta;\mathrm{j}')]$ denotes the local minimum of $\cos\gamma_a$ that occurs at $\cos\gamma_{R2}(\beta=90°)=0.0523$ in Fig. B, which shifts towards the local maximum when one increases β. The first local minimum disappears if $\beta\ge101.45°$.

c) $\cos\gamma_a[\cos\gamma_{R2}(\beta)]<\cos\gamma_a(\gamma_R)\le\cos\gamma_a[\cos\gamma_{R3}(\beta)]$
Where $\cos\gamma_a[\cos\gamma_{R3}(\beta;\mathrm{j}')]$ denotes the value of $\cos\gamma_a$ that coincides with the local maximum $\cos\gamma_a[\cos\gamma_{R1}(\beta)$, but occurs at a larger value of $\cos\gamma_{R3}(\beta)$ than that of

$\cos\gamma_{R2}(\beta)$.The difference between $\cos\gamma_{R3}(\beta)$ and $\cos\gamma_{R2}(\beta)$ decreases when increasing the value of β. The coincidence with the local maximum disappears if $\beta \geq 101.45°$.

d) $\cos\gamma_a[\cos\gamma_{R3}(\beta)] < \cos\gamma_a(\gamma_R) \leq 1$

To facilitate a numerically exact outcome for the integral of the function $F[i, \cos\gamma_a(\cos\gamma_R); \beta, p, j', m_a, \varepsilon', \varepsilon]$ in the range of $90° \leq \beta \leq 101.45°$ of the modified hard shell PES, the integration path is divided into one of three partial integrals, the boundaries of which are chosen according to the prescriptions of a), b) and c) and d). The summation of these partial integrals results in the integrals

$$g^{\mathrm{mod}}_{j=\frac{1}{2},m_a,\varepsilon\to j',m_a,\varepsilon'}(\beta < \beta^{convex}_{\min}, p) \equiv I[i=1; \beta < \beta^{convex}_{\min}, p, j', m_a, \varepsilon', \varepsilon, n=0] \tag{II.8}$$

And

$$C_n(\beta < \beta^{convex}_{\min}, p) \equiv I[\beta < \beta^{convex}_{\min}, p, j', m_a, \varepsilon', \varepsilon, n] \tag{II.9}$$

$$\begin{aligned} I[\beta < \beta^{convex}_{\min}, p, j', m'_a, \varepsilon', n] = \tfrac{2n+1}{2}\Bigg\{ & \int_{-1}^{\cos\{\gamma_a[\cos\gamma_{R1}(\beta)]\}} d\cos\gamma_a \times F[\cos\gamma_a(\cos\gamma_R); \beta < \beta^{convex}_{\min}, p, j', m'_a, \varepsilon', n] + \\ & + \int_{\cos\{\gamma_a[\cos\gamma_{R2}(\beta)]\}}^{\cos\{\gamma_a[\cos\gamma_{R1}(\beta)]\}} d\cos\gamma_a \times F[\cos\gamma_a(\cos\gamma_R); \beta < \beta^{convex}_{\min}, p, j', m'_a, \varepsilon', n] + \\ & + \int_{\cos\{\gamma_a[\cos\gamma_{R2}(\beta)]\}}^{1} d\cos\gamma_a \times F[\cos\gamma_a(\cos\gamma_R); \beta < \beta^{convex}_{\min}, p, j', m'_a, \varepsilon', n] \Bigg\} \end{aligned} \tag{II.10}$$

References:

1. X. Zhang, C. J. Eyles, C. A. Taatjes, D. Ding and S. Stolte, *Physical Chemistry Chemical Physics*, 2013, **15**, 5620-5635.
2. A. Gijsbertsen, H. Linnartz, C. A. Taatjes and S. Stolte, *Journal of the American Chemical Society*, 2006, **128**, 8777-8789.
3. A. Ballast, A. Gijsbertsen, H. Linnartz and S. Stolte, *Molecular Physics*, 2008, **106**, 315-331.
4. C. J. Eyles, M. Brouard, C. H. Yang, J. Kłos, F. J. Aoiz, GijsbertsenA, A. E. Wiskerke and S. Stolte, *Nature Chemistry*, 2011, **3**, 597-602.
5. A. Gijsbertsen, H. Linnartz and S. Stolte, *The Journal of Chemical Physics*, 2006, **125**, 133112-133110.
6. A. Gijsbertsen, H. Linnartz, G. Rus, A. E. Wiskerke, S. Stolte, D. W. Chandler and J. Kłos, *The*

Journal of Chemical Physics, 2005, **123**, 224305-224314.

7. C. J. Eyles, M. Brouard, H. Chadwick, B. Hornung, B. Nichols, C. H. Yang, J. Kłos, F. J. Aoiz, A. Gijsbertsen, A. E. Wiskerke and S. Stolte, *Physical Chemistry Chemical Physics*, 2012, **14**, 5403-5419.
8. M. Brouard, H. Chadwick, C. J. Eyles, B. Hornung, B. Nichols, J. M. Scott, F. J. Aoiz, J. Kłos, S. Stolte and X. Zhang, *Molecular Physics*, 2013, **111**, 1759-1771.
9. J. Kłos, F. J. Aoiz, J. E. Verdasco, M. Brouard, S. Marinakis and S. Stolte, *The Journal of Chemical Physics*, 2007, **127**, 031102-031104.
10. F. J. Aoiz, J. E. Verdasco, M. Brouard, J. Kłos, S. Marinakis and S. Stolte, *J. Phys. Chem. A*, 2009, **113**, 14636-14649.
11. J. Kłos, G. Chalasinski, M. Berry, R. Bukowski and S. Cybulski, *J. Chem. Phys.*, 2000, **112**, 2195-2203.